Biochemistry and Biophysics Reports 37 (2024) 101609

Contents lists available at ScienceDirect

Biochemistry and Biophysics Reports

journal homepage: www.elsevier.com/locate/bbrep

High molecular weight heparin-induced angiogenesis mainly mediated via basic fibroblast growth factor-2- an *in-vivo* (CAM) and *in-silico* analysis

Reji Manjunathan [a,b,*], Kartik Mitra [c], Rahul Vasvani [c], Mukesh Doble [d,**]

[a] Department of Genetics, Dr. Alagappa Mudhaliyar Post Graduate Institute of Basic Medical Science, Taramani Campus, University of Madras, Chennai, 600113, Tamil Nadu, India
[b] Muti-Disciplinary Research Unit, Kottayam Medical College, Kottayam, 686008, Kerala, India
[c] Bioengineering and Drug Design Lab, Department of Biotechnology, Indian Institute of Technology Madras, Chennai, 600036, Tamil Nadu, India
[d] Saveetha Dental College and Hospitals, Saveetha Institute of Medical and Technical Sciences, Chennai, 600077, Tamil Nadu, India

ARTICLE INFO

Keywords:
High-molecular weight heparin
HMWH
Fibroblast growth factor
FGF2
Matrix metalloproteinase 2- MMP2
Molecular docking
Molecular dynamics
Angiogenesis

ABSTRACT

Background: High-molecular weight heparin (HMWH), a molecule extensively used as an anticoagulant, shows concentration-dependent angiogenic and anti-angiogenic potential. So far, no studies have reported the interactive potential of HMWH with various pro-angiogenic growth factors under physiological conditions. Haence, we aimed to find the impact of major pro-angiogenic growth factors under HMWH induced angiogenesis.
Methods: Chicken Chorioallantoic Membranes (CAMs) are incubated with various concentrations of HMWH. Semiquantitative PCR method was implemented to measure the changes in the transcription level of pro-angiogenic growth factors. The scanning electron microscopic technique is applied to find the morphological changes in CAM. Molecular docking and molecular dynamics simulation studies using NAMD and CHARMM force field discerned the heparin-binding mode with the pro-angiogenic growth factors.
Results: HMWH can enhance the transcription level of major pro-angiogenic growth factors, significantly impacting FGF2 under 100 μM concentration. The *in-silico* analysis reveals that HMWH shows the highest binding affinity with FGF2. Further, molecular dynamics and interaction studies using 1 kDa Heparin against FGF2 showed that the former binds stably with the latter due to a strong salt bridge formation between the sulfate groups and arginine residues (ARG 119 and ARG109).
Conclusion: The combined experimental and *in-silico* analysis results reveal that HMWH can interact with pro-angiogenic growth factors under micromolar concentration while inducing angiogenesis. This observation further supports the therapeutic benefits of HMWH as an angiogenic factor under such low concentration. This technique is used to replenish the blood supply to chronic wounds to speed healing and prevent unnecessary amputations.

1. Background

Angiogenesis plays a central role in various physiological and pathological processes such as foetal development, wound healing, and tissue repair after surgery, cancer, and various inflammatory diseases [1]. The process of angiogenesis is highly dynamic and is mediated through a complex multistep process by various cellular components. Proteins such as basic fibroblast growth factor 2 (bFGF2) and vascular endothelial growth factor (VEGF) are associated with endothelial cell (EC) growth and differentiation while on angiogenesis [2,3]. High-molecular-weight Heparin (HMWH) is a highly sulfated glycosaminoglycan carbohydrate molecule. It is commonly used to prevent blood clots in many medical conditions because of its high negative charge density [4,5]. HMWH binds with both angiogenic and anti-angiogenic growth factors through electrostatic interactions due to its polyanionic character and exerts diverse effects on angiogenesis based on the concentration and the molecular weight [6–8]. In the cellular system, the Heparin, which is in the extracellular matrix (ECM), acts as a reservoir for angiogenic growth factors and will sustain a long-term stimulation of endothelial cells in support of neovascularisation [9].

In our previous study, we reported that the HMWH (15 kDa) could

* Corresponding author. Muti-Disciplinary Research Unit, Kottayam Medical College, Kottayam, 686008, Kerala, India.
** Corresponding author.
E-mail addresses: rejimanjunath@gmail.com (R. Manjunathan), mukeshdoble.sdc@saveetha.com (M. Doble).

https://doi.org/10.1016/j.bbrep.2023.101609
Received 6 October 2023; Received in revised form 6 December 2023; Accepted 8 December 2023

induce the formation of capillary-like tubular structures on the chick chorioallantoic membrane vascular model (CAM) and could establish concentration-dependent angiogenic ability. We also pointed out the diffusion pattern and internalised action of Heparin as a preliminary observation, which can further flag the interactive potential of Heparin with many angiogenic growth factors [4]. Hence, in the present study, we aimed to validate the hypothesis that HMWH could regulate angiogenesis by interacting with angiogenic growth factors. For the first time, we evaluated the transcription level of certain pro-angiogenic growth factors and analysed the angiogenic response of HMWH through various methodologies using the CAM vascular model. The CAM is a simple, highly vascularised extra-embryonic membrane that performs multiple embryonic development functions [10]. For more than two decades, the CAM model has used a robust experimental platform to evaluate the angiogenic and anti-angiogenic potential of many natural and synthetic compounds [4,11,12]. In addition, the binding ability of Heparin against these pro-angiogenic growth factors has been probed *in silico* by molecular docking and dynamics simulations using a 1 kDa heparin as a model ligand.

2. Materials and methods

2.1. Materials

Fertilised white leghorn chicken eggs are purchased from Tamil Nadu Poultry Research Station, Madras Veterinary University, Nandanam, Tamil Nadu, India. Gelatine sponges are purchased from Jhonson & Jhonson Pvt Lmtd, India. Paraffin film, wax, TRIzol reagent, agarose, and EtBr are purchased from Sigma, Aldrich, USA. High molecular weight Heparin purchased from CALBIOCHEM, USA (Product No. 375054). ImProm-11™ Reverse Transcriptase kit and GoTaq Green Master Mix PCR amplification kit were from Promega, USA, Oligo (dt) of length 18-meres from Eurofins, mwg operon, Germany, Random hexamers from MP Biomedicals, USA. All primers are purchased from Bioserve, India. DNA ladders purchased from Invitrogen, USA. DAB system purchased from Bangalore Genei, India. Bradford reagent and FITC (Goat ant-rabbit IgG were from Bangalore Genei, India. Rabbit polyclonal FGF2 is a kind gift from Dr. Li Haiqing, MD, Ph.D., Technology transfer specialist, National Cancer Institute, Rockville, USA. Unless otherwise specified, all other common reagents and chemicals are purchased from Sigma, Aldrich, USA.

3. Methods

3.1. Semiquantitative reverse Transcriptase–Polymerase chain reaction (RT-PCR) using CAM vascular bed model

Fertilised white leghorn chicken eggs weighing 50 ± 2 g were incubated at 37 °C in a humidified atmosphere (>60 % relative humidity) based on Hen's Egg Test- Chorioallantoic Membrane (HET-CAM) protocol. On the third day of post-incubation, 2–3 mL of albumin is withdrawn using a 21-gauge needle through the sizeable blunt edge of the eggs to minimise the adhesion of the shell membrane with the CAM. A square window of 1 cm^2 was opened in the eggshell and sealed with paraffin film to prevent dehydration. On day 9, gelatinase sponges of 1 mm^3 in length are placed on the top of the growing CAM under a sterile condition. The sponges are soaked with ten μl of 50, 100, and 150 μM concentrations of Heparin. Control CAM is incubated with ten μl of 1X PBS. The window was closed with transparent adhesive tape, and the eggs were returned for further incubation till day 12 (72 h of incubation), at which the vascularisation potential of CAM reached its maximum. The experiment groups are divided into 4 of, each containing 40 numbers of eggs. Group 1 represents the control; groups 2, 3, and 4 correspond to 10 μL volume of 50, 100, and 150 μM concentrations of Heparin.

According to the manufacturer protocol, total RNA is isolated from the tested CAMs (10 numbers each) using TRIzol reagent (100 mg/1 mL). The isolated RNA's quantity and purity are checked using a UV–visible spectrophotometer. Synthesise of cDNA of 20 μl in volume was done using ImProm-11™ Reverse Transcriptase kit with Oligo (dt) of length 18-meres and random hexamers from 2 μg of RNA. PCR amplification is performed using a Go Taq Green Master Mix kit, and the changes in the level of mRNA expression of FGF2, MMP2, MMP9, NOS, VEGF A, VEGF C, and GAPDH are evaluated using 100 Pico moles of chicken specific primers. The relative expression level of each mRNA transcript is normalised with control. PCR products were subjected to electrophoresis on 1.5 % agarose gel containing 0.5 μg/ml EtBr and were photographed using a Canon Digital Camera of 12X5.0 MegaPixel resolution (Power Shot A95). The base pair products are compared against a DNA ladder of 10 base pairs. The relative density of the bands per experiment is calculated using a Scion Image release α 4.0 3.2 software. Specific primer sequences and the PCR reaction set-up were given in Tables 1 and 2, respectively [13].

3.2. In silico analysis

1 kDa heparin ligand structure was modelled using Marvin, ChemAxon (https://www.chemaxon.com) and energy minimised using MOPAC2016, PM7-a semiempirical force field [14]. The chicken-specific bFGF-2 protein structure was modelled using SWISS MODEL. The chicken bFGF-2 protein sequence (Uniprot:P48844) was used as a query, and the human bFGF-2, PDB:4OEE (sequence identity 91.1 %) was used as a template to build the homology model. The model was validated based on the Ramachandran plot (0 % outlier) and MolProbity score (1.05 Å). The structures for docking were prepared using the UCSF Chimera *dock prep* module [15]. Briefly, the non-receptor atoms were removed, hydrogens were explicitly added, then gasteiger charges were assigned and energy minimised using amff14sb forcefield using steepest descent algorithm with a minimum of 1000 steps. The molecular Docking was performed using Autodock Vina.1.1.2, and the docked poses were clustered using the UCSF Chimera *ensemble/cluster analysis* module. The best binding pose with minimum binding energy was chosen for further molecular simulation. The input files for molecular dynamics simulation were generated using CHARMM-GUI, and the simulations were performed using NAMD.v.2.14 as described elsewhere [16–18]. The equilibration on NVT and NPT were performed for 500 ps each, and the production run was carried out for 50ns. The final simulation trajectories were analysed using VMD.v.1.9.3, and the molecular interactions were visualised using Discovery studio visualiser, BIOVIA, Dassault Systèmes, San Diego [19].

Table 1
Primers sequences.

Gene	Primer Sequence	Base Pair
FGF2	Sense- 5′-TTCTTCCTGCGCATCAAC-3′ Antisense-5′-GGATAGCTTTCTGTCCAG-3′	250 bp
MMP2	Sense- 5′-CCTACACCAAGAACTTCC-3′ Antisense-5′-ACTCCATTCCAAGAATCC-3' (	580 bp
MMP9	Sense-5′-GATGCYCAYTTYGATGATGATGAG-3′ Antisense-5′-GGTCCARTATTTYCCRTYCTTGA-3′	1400 bp
NOS3	Sense- 5′-CCAGAGAGATTCATCTGACCG-3′ Antisense- 5′-GGTCCCTACAACGAGTCTGAA-3′	530 bp
VEGF (165/190)	Sense-5′-GACCCTGGTGGACATTTTCC-3′ Antisense-5′-TGCGCTCGTTTAACTCAAGC-3′	VEGF165 -381 bp VEGF190- 456 bp
GAPDH	Sense- 5′- GAGGAAAGGTCGCCTGGTGGATCG-3′ Antisense-5′-GTGAGGACAAGCAGTGAGGAACG-3′	300 bp

Table 2
The amplification conditions are as follows.

Gene Name	Denaturation	Annealing	Extension	Cycles
FGF2	94 °C/1min	54 °C/1min	72 °C/1min	35
MMP2	94 °C/30sec	60 °C/30sec	72 °C/1min	35
MMP9	94 °C/30sec	48 °C/30sec	72 °C/1min	35
NOS3	94 °C/1min	57 °C/40sec	68 °C/1.5min	30
VEGF(165/190)	94 °C/1min	59 °C/1min	72 °C/1min	40
GAPDH	94 °C/30sec	60 °C/30sec	72 °C/1min	35

4. Immunohistochemistry

CAM tissues incubated with ten μL of 100 μM Heparin (10 μM in thickness) were deparaffinised and dehydrated and allowed to undergo an antigen retrieval process using Sodium Citrate (10 mM-pH 6.0) in a microwave oven for 20 min and washed with DDH2O for 3 × 5 minutes in 1X PBS (pH 7.3). Standard Goat Serum Blocking Solution (2 % goat serum,1 % BSA, 0.1 % cold fish skin gelatin, 0.1 % Triton X-100, 0.05 % Tween- 20, 0.05 % Sodium Azide, 0.01 M PBS (pH 7.2) of 50–75 μL in volume was added immediately on the sections and are incubated for 1 h in a humidified chamber. After washing (IX PBS), the primary antibody of FGF2 was applied on the sections after being diluted in a blocking serum. After overnight incubation, the sections are rinsed with 1X PBS with 0.05 % Tween-20. Diluted FITC (Goat anti-rabbit IgG) and HRP (both Goat anti-rabbit and Goat anti-mouse IgG) secondary antibodies (1:40 dilution) are applied for 1 h according to the manufacturer's instruction. For HRP-conjugated secondary antibodies, the DAB system was used for colour development. The slides were finally counterstained with Mayer's hematoxylin and mounted with 90 % glycerol. For the HRP conjugated system, the images are recorded using a light microscope. For FITC conjugation, the photos are taken using BX51 Olympus Fluorescence Microscope at a wavelength of 515 nm with ASI FISH View 5.5 software at 40× magnification [13].

4.1. Scanning electron microscopic (SEM) analysis

The tested area of the CAM (with 100 μM Heparin) is dissected after 72 h of incubation and washed with 1X PBS. After drying at room temperature, the unfolded air-dried membranes are glued onto stubs with carbon spattered with gold (10 min, 14–17 Ma, and 0.07 m bar). The sections are observed under a Hitachi S–3400 N Variable Pressure Scanning Electron Microscope (Hitachi, Tokyo, Japan) at an accelerating voltage of 15–30 kV, and the images are recorded at 100× magnification [11].

4.2. Data analysis and statistics

Unless otherwise specified, All experiments were performed in triplicate (n = 3). Data are presented as mean ± SEM and are analysed by One-Way ANOVA analysis of variance test, Student's t-test, and Turkey

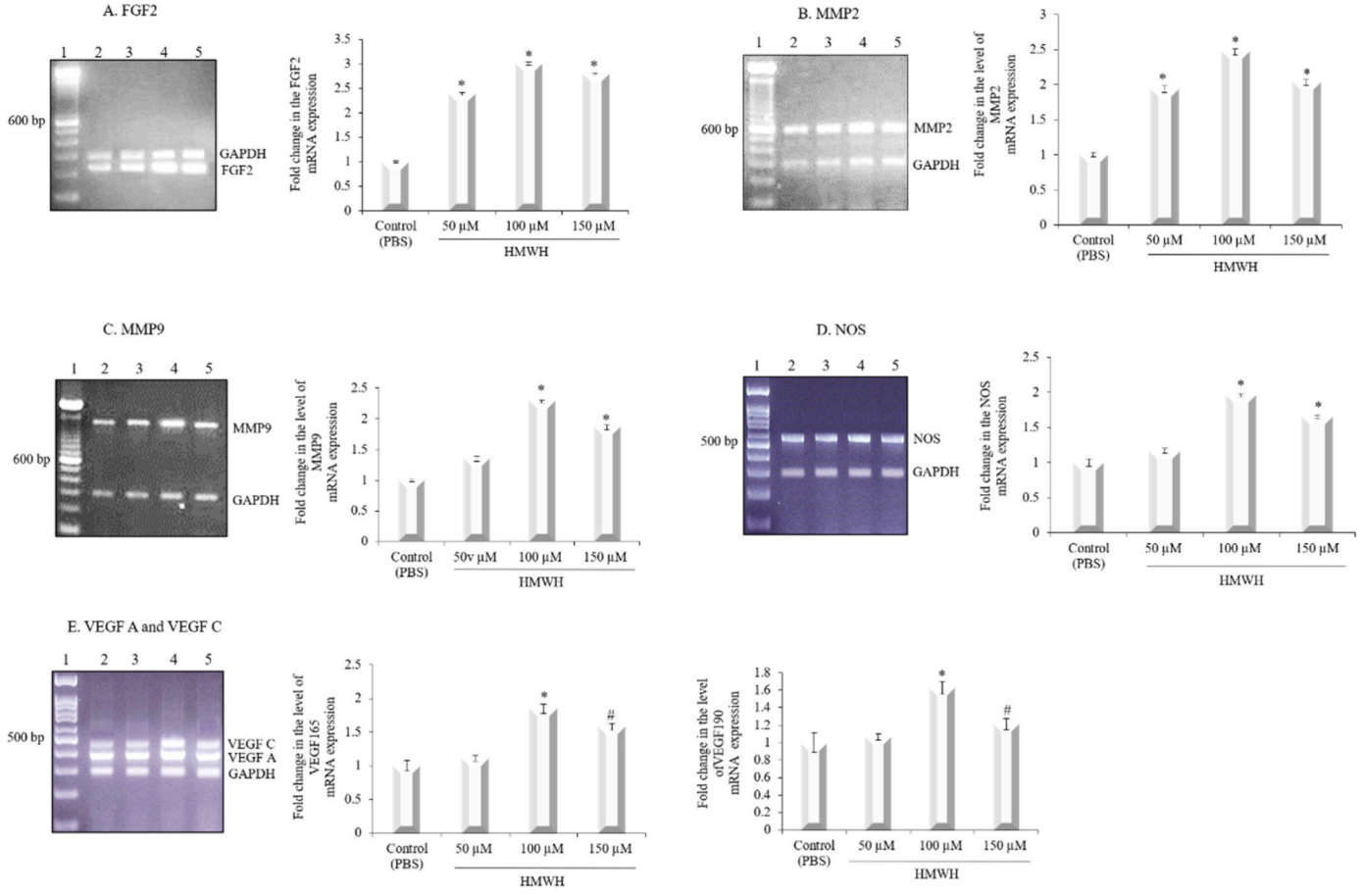

Fig. 1. HMWH up-regulates the molecular level expression of chicken-specific pro-angiogenic growth factors. Images of Reverse Transcriptase - PCR products of **(A)** FGF2, **(B)** MMP2, **(C)** MMP9, **(D)** NOS3, **(E)** VEGF A, and **(F)** VEGF C from CAM after the incubation with 50, 100, and 150 μM concentrations of HMWH for 72 h. Control CAM is incubated with 1X PBS. GAPDH is used as an internal loading control. A 100 bp DNA ladder confirms the transcripts. Graphs represent the OD value ratio of mRNA transcripts after normalising with the GADPH OD value of the same. The OD value is measured using Image J software. The relative level expression of specified genes is increased significantly under all concentrations of HMWH. The relative expression of FGF2 increased significantly under all concentrations of HMWH. Each value is the mean ± SEM, *p=<O.OO1 and #P=O.OO1. Experiments are performed in triplicate, and the data are presented as mean +SEM. (Lane 1 – marker, lane 2- control, lane 3–50 μM HMWH, lane 4–100 μM HMWH, and lane 5–150 μM HMWH).

post hoc tests as appropriate by Sigma Stat 2.0. Values of p = < 0.001 and p = 0.001 were considered statistically significant.

5. Results

5.1. Heparin up-regulates the molecular level expression of pro-angiogenic growth factors

Heparin's potential to enhance the molecular level expression of major pro-angiogenic growth factors such as VEGF 160 (VEGF A), VEGF 190 (VEGF C), FGF2, MMP2, MMP9, and NOS3 were analysed by semiquantitative reverse transcriptase PCR method. The intensity of the bands is measured as relative OD and is given in Fig. 1. The molecular level expression studied pro-angiogenic growth factors are found to increase upon heparin treatment incubation. Heparin at 100 μM exhibits the most significant angiogenic potential among the studied concentrations. When compared to the control value (standardised as one-fold), the mRNA level expression of FGF2 has been found to increase significantly up to 3 fold, MMP2 up to 2.8 fold, MMP9 up to 2.4 fold, NOS3 up to 2.2, VEGF An up to 1.8 fold, and VEGF C up to 1.6 fold under 100 μM concentration of Heparin (*p < 0.001). It is also noted that the mRNA level expression of FGF2 has been increased even at 50 and 150 μM concentrations of Heparin significantly (*p < 0.001). The PCR data support that Heparin could accelerate the transcriptional rate of the pro-angiogenic growth factors while exerting angiogenic potential. Though Heparin is found to increase the transcription level of all the studied pro-angiogenic factors, it is mainly found to increase the molecular level of FGF2 noticeably. The inference also shows that the 100 μM concentration of Heparin shows the maximum angiogenic response among the analysed concentrations.

5.2. Salt bridge formation stabilises bFGF-2 binding with heparin in silico

Since the intact 3D structures of chicken-specific growth factors are not yet available, the homology modelling is adopted using the SWISS-Model to build the models of pro-angiogenic growth factors, namely bFGF2, VEGF-A and VEGF-C. The homology models built were validated based on the Ramachandran plot and GMQE scores, as shown in Fig. 2. The modelling and simulation of 15 kDa-UHMWH Heparin would be computationally intense; hence, the binding interaction analysis here has been studied using a 1 kDa heparin, which consists of the two repeat units of core heparin glycans. The 1 kDa Heparin has been modelled using MOPAC PM7-semi-empirical forcefield. Molecular docking was performed using AutodockVina v.1.2.0. The top 10 poses based on binding energy is clustered, and the ensemble with higher ligand binding pose and minimum binding energy has been selected as the best binding pose.

The docking analysis shows that 1 kDa Heparin exhibits higher affinity towards bFGF2 (−7.0 kcal/mol) than VEGF-A (−6.85 kcal/mol) and VEGF-C (−6.8 kcal/mol) (Fig. 3A). This is inconsistent with our above molecular experimental results which show that the UHMWH exhibits a dose-dependent response increase in FGF2 expression compared to other growth factors such as VEGF-A and VEGF-C. However, the molecular basis for Heparin and bFGF2 interaction has not been explored. To assess Heparin's binding stability and interaction with bFGF2, we performed a 50ns molecular dynamics simulation using NAMD v.2.14 and CHARMM force field.

The FGF2-Heparin (1 kDa) interactions were found to stabilise at 30ns (Fig. 3B) with a minimum average of 6.0 ± 2.0 H-bonds interactions (Fig. 3D) throughout the run. The side chain sulfate group present in Heparin forms a stable salt bridge interaction with Arg-119 and Arg-109, thus stabilising the ligand interactions (Fig. 3E). Previous studies have shown that the affinity of bFGF-2 towards the sulfate moieties plays a significant role in bFGF-2 sequestration by Heparin *in vivo* promoting local enrichment of FGF during neovascularisation [20]. The Heparin binding to bFGFs has also been shown to confer protective effects against proteolytic cleavages [21]. This local enrichment of FGF-2 is considered one of the essential steps in angiogenesis [22]. Although the *in-silico* data presented in this study is based on 1 kDa heparin sulfate, one could imagine that the UHMWH (15 kDa), which is 15-fold larger than 1 kDa Heparin can bind and sequester several bFGF-2 proteins. Khurshid et al. has studied the effect of heparin interaction with amyloid proteins by comparing various molecular weights and observed that the amyloid binding sites of shorter heparin fragments (1 kDa or dp = 4) is similar to larger heparin fragments. However, the longer chains of heparin allowed the self-assembly of amyloids into tertiary structures while the shorter chains formed smaller interspersed heparin-amyloid complexes (https://doi.org/10.1021/acsomega.2c01034). This correlates with the above observed experimental results, where the UHMWH was found to exhibit increased bFGF2 protein levels. These heparins-bFGFs can be released in active form *in vivo* by heparin-degrading enzymes like heparinase I [23].

5.3. Expression of FGF2 elevated in the presence of heparin

From the *in silico* and molecular profiling analysis, we could identify that the heparin-mediated angiogenic process is accelerated through the involvement of FGF2. The inference from the immunohistochemical analysis confirmed the above observation. Fig. 4 represents the level of immunohistochemical expression of FGF2 on the CAM vascular bed. The images indicate that the CAM tissue incubated with 100 μM concentration of Heparin shows more FGF2 in the chorionic layer, majorly at the stromal region than the control CAM (Fig. 4. B). The large blood vessels of the same CAM tissue also show more vessel ECs with FGF2 expression located beneath the chorionic layer. The control CAM shows the presence of more FGF2 by those ECs trapped in the small vessels (Fig. 4. A). The data emphasise that Heparin can induce angiogenesis by enhancing the functional properties of FGF2. These changes, in turn, favour the Heparin-induced microvascular ECs migration, proliferation, and differentiation. FGF2 presence at the vessel endothelium indicates that the Heparin could accelerate the EC activation and sprout to induce new vessels growing from the major ones.

5.4. Heparin changes the microvascular environment of the CAM vascular bed

Observing the changes in the SEM images of the microvascular environment of the CAM vascular bed, we try to confirm the angiogenic potential of Heparin. Fig. 5 represents the SEM images of control CAM and CAM incubated with 100 μM concentration of Heparin. CAM

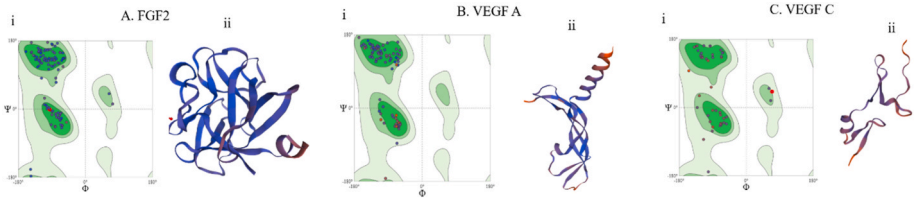

Fig. 2. Ramachandran plot and 3D structures of bFGF2, VEGF A and VEGF C.

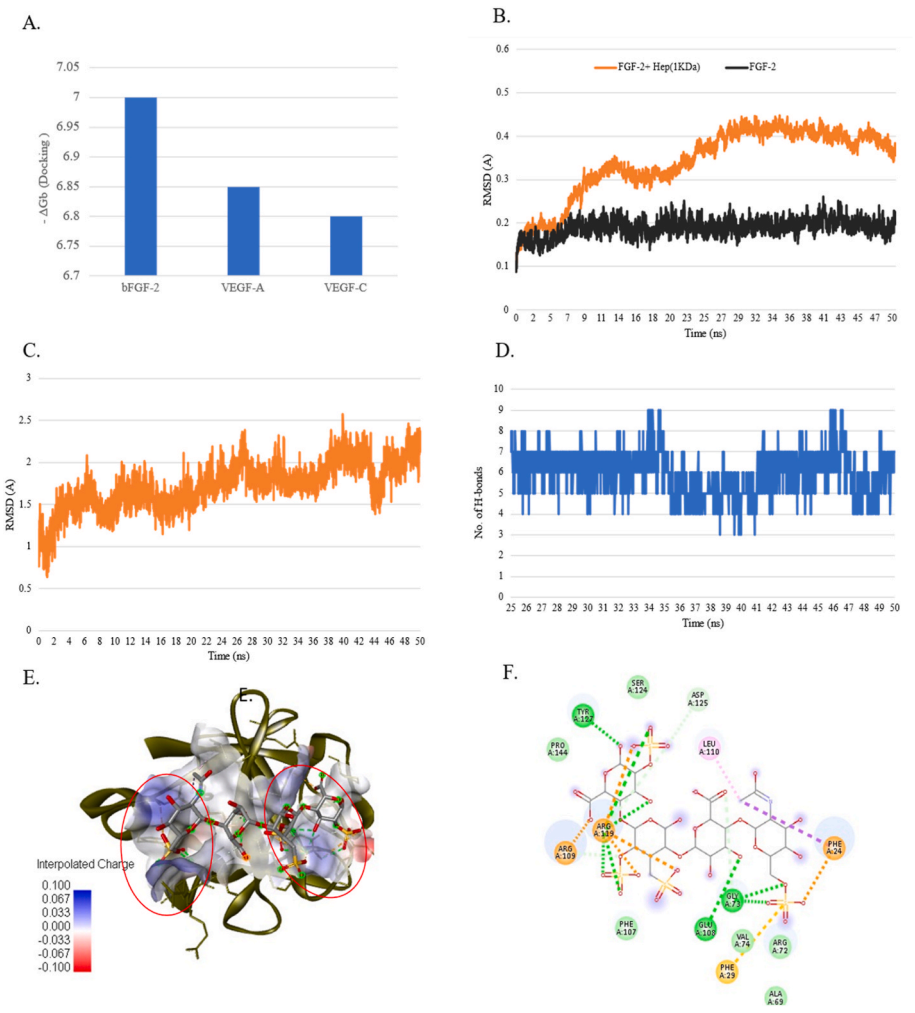

Fig. 3. - A. Docking binding energy of vascular angiogenesis growth factors bFGF2, VEGF-A and VEGF-C against 1 kDa Heparin. B. Protein backbone RMSD analysis of modelled bFGF-2 alone(black) and bFGF2+heparin(1 kDa) (orange) during the molecular dynamics production run; C. RMSD of ligand (1 kDa-heparin) concerning protein backbone; D. Total hydrogen bond interaction count of Heparin and bFGF2 during run; E. Post 50ns snapshot of Heparin (1 kDa)-bFGF2 interaction. The protein surface represents the charge density. The red circle highlights the regions of salt bridge formation between sulfate groups of heparins and Arg 119 and Arg109 residues; F—the ligand interaction plot of the heparin-bFGF2 complex. (For interpretation of the references to colour in this figure legend, the reader is referred to the Web version of this article.)

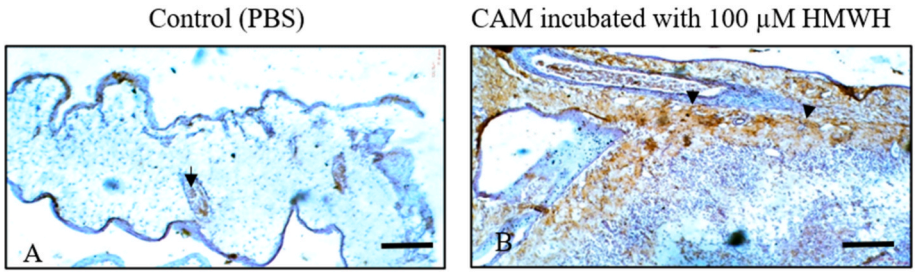

Fig. 4. HMWH up-regulates the protein level expression of FGF2 Immunohistochemical images of CAM with FGF2 4 expression after the incubation with 100 µM concentration of HMWH for 72 h. Control CAM is incubated with 1X PBS. Control CAM shows the presence of FGF2 in ECs trapped at the small vessels (Fig. 4. A). CAM incubated with 100 µM concentration of HMWH shows the presence of FGF2 in the chorionic layer, majorly at the stromal region and by ECs trapped at large and small vessels (Fig. 4. B). Images are recorded by light and BX51 Olympus fluorescence microscopes. The arrow indicates the presence of protein, the magnification is 60×, and the magnification bar is 50 µm.

vascular bed incubated with Heparin shows many sprouted and elongated vessels (black arrows) with a few angiogenic holes (yellow arrows). The capillaries are visible as septum-like structures without circular posts near the giant vessel (red arrow) because of long tissue septa from the capillary plexus that separates the blood vessels. On the contrary, control CAM shows a flat capillary network at the outer structure with small blood vessel bulges (green arrows). Angiogenic holes (yellow arrows) are also visible as an indication of intussusceptive angiogenesis, which usually happens during CAM vasculature development. Thus, SEM image analysis supports the fact that Heparin can

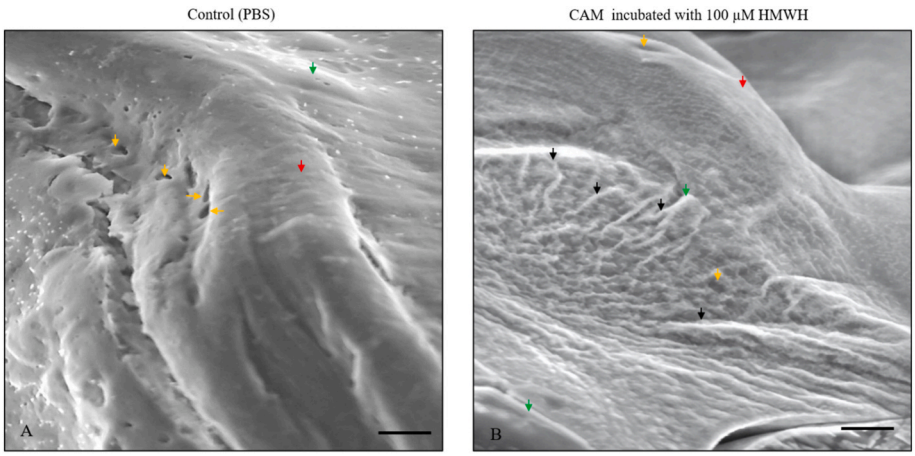

Fig. 5. HMWH modifies the micro-vascular structure of the CAM vascular bed. Scanning electron microscopic images of CAM incubated with 100 µM concentration of HMWH and control CAM with 1X PBS for 72 h. CAM set with HMWH (Fig. 5. B) shows the presence of many sprouted and elongated vessels (black arrows) with a few angiogenic holes (yellow arrows). The capillaries resemble septum-like structures near the giant vessel (red arrow). Control CAM (Fig. 5. A) shows a flat capillary network at the outer frame with small blood vessel bulges (green arrows) with many angiogenic holes (yellow arrows) as an indication of intussusceptive angiogenesis for the normal development of CAM vasculature. HMWH can potentially induce the sprouting of new blood vessels from the main vessel through EC elongation and migration. Images represent three sets of experiments, and the magnification bar is 200 µm. (For interpretation of the references to colour in this figure legend, the reader is referred to the Web version of this article.)

induce the sprouting of new blood vessels from the main vessel through EC elongation and migration.

6. Discussion

Our earlier study reported that HMWH (15 kDa) could exhibit concentration-dependent neovascularisation potential on the CAM vascular bed. The molecule significantly induced the vessels' growth and was found to increase the thickness of the vascular bed due to enhanced neovascularisation at the area of incubation under 100 µM concentration. In the research, we also pointed out the diffusion pattern and internalised action of Heparin as a preliminary observation, which can further flag the interactive potential of Heparin with many angiogenic growth factors [4]. Hence, in the present study, we aimed to validate the angiogenic potential of HMWH and its potential to interact with the main pro-angiogenic growth factors. For the first time, we evaluated the transcription level of certain pro-angiogenic growth factors and analysed the angiogenic response of HMWH through various methodologies using the CAM vascular model.

Heparin is known for its diverse effect on angiogenesis [21,22]. Heparin can bind with vascular cells such as ECs and smooth muscle cells and regulate the various angiogenic processes. Heparin interaction with angiogenic growth factors depends on the distribution of sulfate groups and the length of the distinct oligosaccharide sequences [23]. Our mRNA expression study reveals that HMWH could show dose-dependent interaction with major pro-angiogenic growth factors. Among the studied concentrations, 100 µM of Heparin exerts its maximum potential by significantly increasing the mRNA level of main pro-angiogenic growth factors. The transcription level of FGF2 has elevated substantially under all three concentrations of HMWH with a greater transcription rate at 100 µM concentration. FGF2 directly affects angiogenesis through the induction of tubulogenesis and migration of endothelial progenitor cells and affects the expression of several chemo cytokines, such as VEGFs. Our study found that the micromolar concentration of HMWH can accelerate the gene transcription level of FGF2 significantly more than any other analysed growth factors.

Molecular docking analysis is performed to understand the binding interaction of Heparin with main pro-angiogenic growth factors using 1 kDa Heparin. The docking data agrees that Heparin could exhibit a higher affinity towards bFGF2 (−7.0 kcal/mol) than studied pro-angiogenic growth factors. The observation is in accordance with the molecular profiling of pro-angiogenic growth factors under high molecular weight heparin. The molecular dynamic study further cemented the notion that the molecule FGF2 could form a minimum average of 6.0 ± 2.0 hydrogen bonds, and the side chain sulfate group of Heparin creates a stable salt bridge interaction with Arg-119 and Arg 109. This bonding further stabilised the interaction between Heparin and FGF2. The finding further cemented the greater affinity of FGF2 molecules with the sulfate moiety and its protection impact against proteolytic cleavage [20,21]. The high binding affinity of Heparin with FGF2 further supported the transportation and release of FGF2 at its specific stage to initiate its biological function [4,23].

The CAM consists of a dense vascular network, and this extra embryonic membrane physiologically serves as a respiratory organ for the embryo until it hatches. Because of its extensive vasculature, CAM allows a large-scale screening of chemicals that impact angiogenesis with the easy application of many experimental methodologies [10]. One of the main advantages of CAM is that the impact of the test materials on angiogenesis can be visualised directly and could be validated further with the aid of many microscopic applications [4]. In this study, we analysed the changes in the vascular morphological structure of the CAM under HMWH incubation. We found that the HMWH can induce neovascularisation by employing numerous small vessels from the main large blood vessels. Involvement of the specific growth factor, such as FGF2-induced angiogenesis, is documented by identifying the molecules' protein level expression on CAM. The data shows that the word FGF2 is more prominent in CAM incubated with HMWH. The FGF2 expression is evident in those ECs trapped at the main blood vessels and between the main vessels' septum, in which the sprouting of new blood vessels occurs.

7. Conclusion

The results obtained from our combined experimental and molecular modelling approach provide precious information on how HMWH (15 kDa) interacts with various pro-angiogenic growth factors under various concentrations while inducing angiogenesis. The neovascularisation potential of HMWH is concentration-dependent and exerts its maximum angiogenic potential at micromolar concentration. HMWH can accelerate the transcription level of most known pro-angiogenic growth factors, but it significantly activates the angiogenic process through FGF2. Through *in-silico* modelling, we also demonstrate that Heparin and

bFGF-2 interaction is stabilised by salt bridge formation between the arginine residues in bFGF2 and anionic sulfate groups in Heparin. The significance of these findings can be implicated in exploring the pro-angiogenic therapeutic potential of UHMWH. It also highlights that this can be a suitable biomaterial for *in vivo* growth factor delivery. Applying this molecule for the prevention of various pathological conditions that arise due to insufficient healthy vasculatures, such as wound healing.

Ethics approval and consent to participate

Not applicable.

Availability of data and materials

This published article includes all the data generated or analysed during this study.

Funding

No funds, grants, or other support are received for this study.

Author's contribution

RM designed the work, carried out the experimental studies and made the manuscript. KM and RV performed the molecular docking and dynamics analysis and wrote the manuscript. MD reviewed the manuscript. All the authors have read and approved the manuscript.

CRediT authorship contribution statement

Reji Manjunathan: Conceptualization, Formal analysis, Investigation, Methodology, Validation, Visualization, Writing – original draft, Writing – review & editing. **Kartik Mitra:** Formal analysis, Software, Validation. **Rahul Vasvani:** Formal analysis, Software. **Mukesh Doble:** Formal analysis, Methodology, Software, Supervision.

Declaration of competing interest

The authors declare no interest.

Data availability

Data will be made available on request.

Acknowledgement

We want to thank Dr. Li Haiqing, MD, Ph.D., -Technology transfer specialist, National Cancer Institute, Rockville, USA, for the gift of Rabbit polyclonal FGF2 antibody. RV thanked NPTEL for the project internship opportunity.

Abbreviations

HMWH	High molecular weight heparin
CAM	Chorioallantoic Membrane
PCR	Polymerase Chain Reaction
EC	Endothelial Cell
ECM	Extra Cellular Matrix

References

[1] S.Y. Yoo, S.M. Kwon, Angiogenesis and its therapeutic opportunities, Mediators Inflamm 2013 (2013), 127170, https://doi.org/10.1155/2013/127170. PMID: 23983401; PMCID: PMC3745966.

[2] W.H. Burgess, T. Maciag, The heparin-binding (fibroblast) growth factor family of proteins, Annu. Rev. Biochem. 58 (1989) 575–606, https://doi.org/10.1146/annurev.bi.58.070189.003043. PMID: 2549857.

[3] A. Hoeben, B. Landuyt, M.S. Highley, H. Wildiers, A.T. Van Oosterom, E.A. De Bruijn, Vascular endothelial growth factor and angiogenesis, Pharmacol. Rev. 56 (4) (2004 Dec) 549–580, https://doi.org/10.1124/pr.56.4.3.PMID:15602010.

[4] R.B. Rema, K. Rajendran, M. Ragunathan, Angiogenic efficacy of Heparin on chick chorioallantoic membrane, Vasc. Cell 4 (1) (2012 Apr 18) 8, https://doi.org/10.1186/2045-824X-4-8. PMID: 22513007; PMCID: PMC3514200.

[5] E. Gray, B. Mulloy, T.W. Barrowcliffe, Heparin and low-molecular-weight heparin, Thromb Haemost 99 (5) (2008 May) 807–818, https://doi.org/10.1160/TH08-01-0032. PMID: 18449410.

[6] A. Nawaz, S. Zaman Safi, S. Sikandar, R. Zeeshan, S. Zulfiqar, N. Mehmood, H. M. Alobaid, F. Rehman, M. Imran, M. Tariq, A. Ali, T.B. Emran, M. Yar, Heparin-loaded Alginate hydrogels: Characterisation and molecular Mechanisms of Their angiogenic and anti-Microbial potential, Materials 15 (19) (2022 Sep 26) 6683, https://doi.org/10.3390/ma15196683. PMID: 36234025; PMCID: PMC9573464.

[7] J. Rak, J.I. Weitz, Heparin and angiogenesis: size matters, Arterioscler. Thromb. Vasc. Biol. 23 (11) (2003 Nov 1) 1954–1955, https://doi.org/10.1161/01.ATV.0000100563.16983.19.PMID:14617616.

[8] W. Cheng, F.Z. Dahmani, J. Zhang, H. Xiong, Y. Wu, L. Yin, J. Zhou, J. Yao, Anti-angiogenic activity and antitumor efficacy of amphiphilic twin drug from ursolic acid and low molecular weight heparin, Nanotechnology 28 (7) (2017 Feb 17), 075102, https://doi.org/10.1088/1361-6528/aa53c6. Epub 2017 Jan 16. PMID: 28091396.

[9] N.N. Nissen, R. Shankar, R.L. Gamelli, A. Singh, L.A. DiPietro, Heparin and heparan sulphate protect basic fibroblast growth factor from non-enzymic glycosylation, Biochem. J. (Pt 3) (1999) 338. Pt 3):637-642. PMID: 10051433; PMCID: PMC1220097.

[10] P. Nowak-Sliwinska, T. Segura, M.L. Iruela-Arispe, The chicken chorioallantoic membrane model in biology, medicine and bioengineering, Angiogenesis 17 (4) (2014 Oct) 779–804, https://doi.org/10.1007/s10456-014-9440-7. Epub 2014 Aug 20. PMID: 25138280; PMCID: PMC4583126.

[11] R. Manjunathan, M. Ragunathan, In ovo administration of human recombinant leptin shows dose-dependent angiogenic effect on chicken chorioallantoic membrane, Biol. Res. 48 (1) (2015 Jun 10) 29, https://doi.org/10.1186/s40659-015-0021-z. PMID: 26060038; PMCID: PMC4470073.

[12] R. Manjunathan, M. Ragunathan, Evaluation of Antiangiogenic potential of MMP2 Antisense Oligonucleotide for the Management of proliferative Diabetic Retinopathy using chicken chorioallantoic membrane, Mol Biol 5 (2016) 148.

[13] R. Manjunathan, M. Ragunathan, Chicken chorioallantoic membrane as a reliable model to evaluate osteosarcoma-an experimental approach using SaOS2 cell line, Biol. Proced. Online 17 (2015 Jun 6) 10, https://doi.org/10.1186/s12575-015-0022-x. PMID: 26109911; PMCID: PMC4479062.

[14] J.J. Stewart, Optimisation of parameters for semiempirical methods VI: more modifications to the NDDO approximations and re-optimisation of parameters, J. Mol. Model. 19 (1) (2013 Jan) 1–32, https://doi.org/10.1007/s00894-012-1667-x. Epub 2012 Nov 28. PMID: 23187683; PMCID: PMC3536963.

[15] E.F. Pettersen, T.D. Goddard, C.C. Huang, G.S. Couch, D.M. Greenblatt, E.C. Meng, T.E. Ferrin, UCSF Chimera–a visualisation system for exploratory research and analysis, J. Comput. Chem. 25 (13) (2004 Oct) 1605–1612, https://doi.org/10.1002/jcc.20084.PMID:15264254.

[16] R. Manjunathan, V. Periyaswami, K. Mitra, A.S. Rosita, M. Pandya, J. Selvaraj, L. Ravi, N. Devarajan, M. Doble, Molecular docking analysis reveals the functional inhibitory effect of Genistein and Quercetin on TMPRSS2: SARS-COV-2 cell entry facilitator spike protein, BMC Bioinf. 23 (1) (2022 May 16) 180, https://doi.org/10.1186/s12859-022-04724-9. PMID: 35578172; PMCID: PMC9108711.

[17] J. Lee, X. Cheng, J.M. Swails, M.S. Yeom, P.K. Eastman, J.A. Lemkul, S. Wei, J. Buckner, J.C. Jeong, Y. Qi, S. Jo, V.S. Pande, D.A. Case, C.L. Brooks 3rd, A. D. MacKerell Jr., J.B. Klauda, W. Im, CHARMM-GUI input generator for NAMD, GROMACS, AMBER, OpenMM, and CHARMM/OpenMM simulations using the CHARMM36 additive force field, J Chem Theory Comput 12 (1) (2016 Jan 12) 405–413, https://doi.org/10.1021/acs.jctc.5b00935. Epub 2015 Dec 3. PMID: 26631602; PMCID: PMC4712441.

[18] J.C. Phillips, D.J. Hardy, J.D.C. Maia, J.E. Stone, J.V. Ribeiro, R.C. Bernardi, R. Buch, G. Fiorin, J. Hénin, W. Jiang, R. McGreevy, M.C.R. Melo, B.K. Radak, R. D. Skeel, A. Singharoy, Y. Wang, B. Roux, A. Aksimentiev, Z. Luthey-Schulten, L. V. Kalé, K. Schulten, C. Chipot, E. Tajkhorshid, Scalable molecular dynamics on CPU and GPU architectures with NAMD, J. Chem. Phys. 153 (4) (2020 Jul 28), 044130, https://doi.org/10.1063/5.0014475. PMID: 32752662; PMCID: PMC7395834.

[19] W. Humphrey, A. Dalke, K. Schulten, VMD: visual molecular dynamics, J. Mol. Graph. 14 (1) (1996 Feb) 33–38, 27-38. doi: 10.1016/0263-7855(96)00018-5. PMID: 8744570.

[20] I. Vlodavsky, G. Korner, R. Ishai-Michaeli, P. Bashkin, R. Bar-Shavit, Z. Fuks, Extracellular matrix-resident growth factors and enzymes: possible involvement in tumour metastasis and angiogenesis, Cancer Metastasis Rev. 9 (3) (1990 Nov) 203–226, https://doi.org/10.1007/BF00046361.PMID:1705486.

[21] A. Sommer, D.B. Rifkin, Interaction of Heparin with human basic fibroblast growth factor: protection of the angiogenic protein from proteolytic degradation by a

glycosaminoglycan, J. Cell. Physiol. 138 (1) (1989 Jan) 215–220, https://doi.org/10.1002/jcp.1041380129.PMID:2910884.

[22] H.R. Seo, H.E. Jeong, H.J. Joo, S.C. Choi, C.Y. Park, J.H. Kim, J.H. Choi, L.H. Cui, S. J. Hong, S. Chung, D.S. Lim, Intrinsic FGF2 and FGF5 promote the angiogenesis of human aortic endothelial cells in a 3D microfluidic angiogenesis system, Sci. Rep. 6 (2016 Jun 30), 28832, https://doi.org/10.1038/srep28832. PMID: 27357248; PMCID: PMC4928073.

[23] A. Nilasaroya, P.J. Martens, J.M. Whitelock, Enzymatic degradation of heparin-modified hydrogels and its effect on bioactivity, Biomaterials 33 (22) (2012 Aug) 5534–5540, https://doi.org/10.1016/j.biomaterials.2012.04.022. Epub 2012 May 8. PMID: 22575836.